

# c-Src but Not Fyn Promotes Proper Spindle Orientation in Early Prometaphase\*<sup>§</sup>

Received for publication, January 10, 2012, and in revised form, May 30, 2012. Published, JBC Papers in Press, June 11, 2012, DOI 10.1074/jbc.M112.341578

Yuji Nakayama<sup>1</sup>, Yuki Matsui, Yumi Takeda, Mai Okamoto, Kohei Abe, Yasunori Fukumoto, and Naoto Yamaguchi<sup>2</sup>

From the Department of Molecular Cell Biology, Graduate School of Pharmaceutical Sciences, Chiba University, Chiba 260-8675, Japan

**Background:** Src family tyrosine kinases have been reported to activate in mitosis and associate with the mitotic spindle.

**Results:** Reintroduction of c-Src but not Fyn rescues spindle misorientation and facilitates astral microtubule regrowth from depolymerization.

**Conclusion:** c-Src is involved in spindle orientation through the centrosome-mediated pathway for spindle formation.

**Significance:** Our results provide the first demonstration of a role for c-Src in mitotic spindle orientation.

Src family tyrosine kinases (SFKs) participate in mitotic signal transduction events, including mitotic entry, cleavage furrow ingression, and cytokinesis abscission. Although SFKs have been shown to associate with the mitotic spindle, the role of SFKs in mitotic spindle formation remains unclear. Here, we show that c-Src promotes proper spindle orientation in early prometaphase. Src localizes close to spindle poles in a manner independent of Src kinase activity. Three-dimensional analyses showed that Src inhibition induced spindle misorientation, exhibiting a tilting spindle in early prometaphase. Spindle misorientation is frequently seen in SYF cells, which harbor triple knock-out mutations of c-Src, c-Yes, and Fyn, and reintroduction of c-Src but not Fyn into SYF cells rescued spindle misorientation. Spindle misorientation was also observed upon Src inhibition under conditions in which Aurora B was inhibited. Inducible expression of c-Src promoted a properly oriented bipolar spindle, which was suppressed by Src inhibition. Aster formation was severely inhibited in SYF cells upon Aurora B inhibition, which was rescued by reintroduction of c-Src into SYF cells. Furthermore, reintroduction of c-Src facilitated microtubule regrowth from cold-induced depolymerization and accelerated M phase progression. These results suggest that c-Src is involved in spindle orientation through centrosome-mediated aster formation.

Cell division is a process to equally separate replicated chromosomes into two daughter cells. Deregulation of cell division results in gain or loss of chromosomes, leading to tumorigene-

sis. Faithful chromosome segregation depends on proper mitotic spindle functions, and tight control of dynamics of spindle microtubules prevents malignant tumor progression.

The centrosome is the primary microtubule-organizing center in animal cells. Chromosomes can promote spindle assembly through the self-organization model (1, 2). However, in the absence of centrosomes, mitotic spindles are frequently misoriented due to loss of astral microtubules, and spindle misorientation leads to a decrease in the fidelity of cytokinesis (3). Thus, the centrosome is important in ensuring mitotic fidelity (4). Aurora A is a member of the Aurora family of Ser/Thr kinases and plays a variety of roles in centrosome maturation for setting up the mitotic spindle (5–8). The other member, Aurora B, has a critical role in regulation of chromosome interactions with microtubules, chromatid cohesion, spindle stability, and cytokinesis (8, 9). Small molecule inhibitors of Aurora kinases have been used to dissect the signaling pathways that are orchestrated by Aurora kinases. ZM447439, a specific inhibitor of Aurora A and Aurora B, strongly interferes with mitotic spindle assembly by inhibiting the formation of microtubules that are nucleated by chromatin (10).

Src family tyrosine kinases (SFKs)<sup>3</sup> consist of eight members (c-Src, Lyn, Fyn, c-Yes, Lck, c-Fgr, Hck, and Blk), and they have crucial roles in cell proliferation, adhesion, migration, and development (11, 12). Multiple combinations in expression of each SFK member have been shown to serve specific and overlapping functions. SFKs are also known to regulate cell division because SFK inhibitors cause cell division defects (13–15). Microinjection of anti-Src antibody into G<sub>2</sub> cells prevents mitotic entry (16), and that of anti-Src antibody or the SFK SH2 (Src homology 2) domain after nuclear envelope breakdown has been reported to block cytokinesis (14, 17). Furthermore, the specific Src family kinase inhibitor PP2 (18) inhibits cytokinesis, which is also prevented by the MEK inhibitor U0126 (15), suggesting a role of the Src/MEK/ERK pathway in regulation of cytokinesis. The kinase activities of SFKs are up-regulated upon mitotic entry through Cdk1-induced phosphorylation of the unique domain of SFKs, which promotes dephosphorylation of the C-terminal inhibitory tyrosine residue (19–23). Although

\* This work was supported in part by grants-in-aid for scientific research and special funds for education and research (Development of SPECT Probes for Pharmaceutical Innovation) from the Japanese Ministry of Education, Culture, Sports, Science, and Technology; a research grant from the Mochida Memorial Foundation for Medical and Pharmaceutical Research; and a research grant from the Nanohana Competition 2011 Award of Chiba University and the Futaba Electronics Memorial Foundation (to Y. F.).

<sup>§</sup> This article contains supplemental Figs. S1 and S2.

<sup>1</sup> To whom correspondence may be addressed: Dept. of Molecular Cell Biology, Graduate School of Pharmaceutical Sciences, Chiba University, Inohana 1-8-1, Chuo-ku, Chiba 260-8675, Japan. Tel./Fax: 81-43-226-2869; E-mail: nakayama@p.chiba-u.ac.jp.

<sup>2</sup> To whom correspondence may be addressed. Tel./Fax: 81-43-226-2868; E-mail: nyama@faculty.chiba-u.jp.

<sup>3</sup> The abbreviation used is: SFK, Src family tyrosine kinase.

## Src Signaling Promotes Spindle Formation

SFKs are involved in the regulation of mitotic entry and cytokinesis, the precise roles of SFKs in cell division are not fully understood.

Association of SFKs with the mitotic spindle has been reported. In mouse development, activated SFKs are strongly associated with the meiotic spindle at all stages of meiosis (24). A non-myristoylated c-Src mutant associates with the mitotic spindle and spindle poles in NIH 3T3-derived cells (25). Fyn is localized at the mitotic spindle in human T lymphocytes (26) and rat eggs (27). Triton X-100-insoluble Lyn is associated with the mitotic spindle in human immature myeloid cells (28). Furthermore, inhibition of SFKs causes formation of disorganized spindles in rat eggs (27). However, the role of SFKs in mitotic spindle formation remains unknown. Therefore, we wished to explore the function of SFKs in mitotic spindle formation.

In this study, we show that activation of c-Src promotes proper spindle orientation through centrosome-mediated spindle formation. Our results provide the first demonstration of a mitotic role for c-Src in mammalian cells.

### EXPERIMENTAL PROCEDURES

**Plasmids**—To construct the pcDNA4/TO/c-Src-HA vector for inducible expression of c-Src-HA, the HindIII-XhoI fragment of pcDNA3/c-Src-HA (provided by S. A. Laporte) (29) was subcloned into the HindIII-XhoI site of pcDNA4/TO/neoR (30). By sequencing the resulting construct, a mutation was found at Leu<sup>175</sup>. To remove the mutation, the NotI-KpnI fragment was replaced with the NotI-KpnI fragment of cDNA encoding human c-Src (provided by D. J. Fujita) (31).

**Chemicals**—PP2 (Calbiochem), SU6656 (Sigma), U0126 (Calbiochem), RO-3306 (Calbiochem), and ZM447439 (JS Research Chemicals Trading) were dissolved in dimethyl sulfoxide. A list of inhibitors used in this study is provided in supplemental Fig. S1.

**Cells and Transfection**—HeLa and HeLa S3 cells (Japanese Collection of Research Bioresources, Osaka, Japan) were cultured in Iscove's modified Dulbecco's medium containing 1% FBS and 4% bovine serum. SYF cells harboring triple knock-out mutations of c-Src, c-Yes, and Fyn (32); c-Src-reintroduced SYF (SYF/c-Src) cells (33); and Fyn-reintroduced SYF (SYF/Fyn) cells were cultured in Iscove's modified Dulbecco's medium containing 5% FBS. Transfection was performed using linear polyethylenimine (25 kDa; Polysciences, Inc.) (34). To generate a stable cell line for tetracycline-inducible c-Src overexpression, HeLa S3 cells were cotransfected with pCAG/TR (35) and a plasmid containing the hygromycin resistance gene and selected in 200  $\mu$ g/ml hygromycin (Wako Pure Chemical Industries, Ltd, Osaka). Expression of the tetracycline repressor in cell clones was confirmed by Western blotting using anti-tetracycline repressor antibody. Tetracycline repressor-expressing HeLa S3 cells (clone A3f5) were transfected with pcDNA4/TO/c-Src-HA and selected in 200  $\mu$ g/ml G418 (clone A5e5). Inducible c-Src-overexpressing cells were generated from tetracycline repressor-expressing HeLa cells (Src45 cells) (37). Doxycycline, a tetracycline derivative, was used at 1  $\mu$ g/ml for c-Src overexpression. To generate the add-back version of SYF cells re-expressing c-Src or Fyn, SYF cells were transfected

with pcDNA4/TO/c-Src (37) or pcDNA4/TO/Fyn (38) and selected in 333  $\mu$ g/ml Zeocin (Invitrogen).

**Cell Synchronization**—To synchronize exponentially growing cells at M phase, cells were treated with 4 mM thymidine for 24 h. After washing with PBS, cells were released into prewarmed drug-free fresh medium and cultured for 6 h. The cells were then incubated with 6–10  $\mu$ M RO-3306 for 10 h to arrest cells at late G<sub>2</sub> phase. G<sub>2</sub>-arrested cells were washed with PBS supplemented with Ca<sup>2+</sup> and Mg<sup>2+</sup> and released into prewarmed fresh medium. Mitotic cells were collected by mitotic shake-off. Alternatively, exponentially growing cells were treated with 8–9  $\mu$ M RO-3306 for 20 h without thymidine treatment, and mitotic cells were collected by mitotic shake-off after release from G<sub>2</sub> arrest.

**Antibodies**—Mouse monoclonal anti-v-Src (clone 327, Calbiochem), anti-Src (clone GD11, Millipore), anti-Src phospho-Tyr<sup>416</sup> (phospho-Src family, BioSource), anti-phosphotyrosine (clone 4G10, Upstate Biotechnology), anti-phospho-p44/42 MAPK Thr<sup>202</sup>/Tyr<sup>204</sup> (phospho-ERK1/2; clone E10, New England Biolabs), anti-IAK1 (Aurora A; clone 4, BD Biosciences), anti-AIM-1 (Aurora B; clone 6, BD Biosciences), and anti-phospho-histone H3 Ser<sup>10</sup> (clone 6G3, Millipore) antibodies; rabbit polyclonal anti-ERK2 (clone C-14, Santa Cruz Biotechnology), anti-phospho-Aurora A Thr<sup>288</sup>/Aurora B Thr<sup>232</sup>/Aurora C Thr<sup>198</sup> (clone D13A11, Cell Signaling Technology), and anti-cyclin B1 (clone H-433, Santa Cruz Biotechnology) antibodies; and rat monoclonal anti- $\alpha$ -tubulin antibody (clone MCA78G, Serotec) were used. Horseradish peroxidase-conjugated F(ab')<sub>2</sub> fragments of anti-mouse IgG antibody, anti-rabbit IgG antibody, and anti-rat IgG antibody (GE Healthcare) and peroxidase-conjugated anti-mouse IgG light chain antibody (Jackson ImmunoResearch Laboratories) were used. Alexa Fluor 488-conjugated donkey anti-mouse IgG (Invitrogen) and anti-rat IgG (Invitrogen) antibodies were used.

**Immunofluorescence Microscopy**—Immunofluorescence staining was performed as described (36, 39–43). In brief, cells were fixed in PBS containing 4% paraformaldehyde for 20 min or in PTEMF buffer (20 mM PIPES (pH 6.9), 0.2% Triton X-100, 10 mM EGTA, 1 mM MgCl<sub>2</sub>, and 4% paraformaldehyde) for 20 min at 37 °C. Fixed cells were permeabilized and blocked in PBS containing 0.1% saponin and 3% bovine serum albumin and then sequentially incubated with a primary and a secondary antibody for 1 h each. DNA was stained with 10–50  $\mu$ g/ml propidium iodide for 30 min after treatment with 200  $\mu$ g/ml RNase A. Confocal and Nomarski-differential interference contrast images were obtained using an LSM 510 laser-scanning microscope with a  $\times$  40/1.2 numerical aperture water-, a  $\times$  63/1.4 oil-, or a  $\times$  100/1.3 oil-immersion objective (Zeiss). Composite figures were prepared using Photoshop 11.0 and Illustrator 14.0 software (Adobe).

**Microtubule Regrowth Assay**—SYF and SYF/c-Src cells were incubated on ice for 4 h to completely depolymerize microtubules (44). After cells were returned to 37 °C for 90 s, cells were fixed in 100% methanol at –30 °C for 5 min and stained for  $\alpha$ -tubulin and DNA. The integrated fluorescence intensity of  $\alpha$ -tubulin staining of cells, which shows aster formation, was measured in a circle centered on the centrosome with a radius of 1.5  $\mu$ m using NIH ImageJ software.

**Western Blotting**—Cells lysates were separated by SDS-PAGE and electrotransferred onto PVDF membranes (Millipore). To examine the phosphorylation status of proteins, cell lysates were prepared with SDS sample buffer containing phosphatase inhibitors (20 mM  $\beta$ -glycerophosphate, 50 mM NaF, and 10 mM sodium orthovanadate). Immunodetection was performed as reported previously (30, 38, 45, 46). Sequential re-probing of membranes with a variety of antibodies was performed after the complete removal of primary and secondary antibodies from membranes in stripping buffer or inactivation of HRP with 0.1%  $\text{NaN}_3$  according to the manufacturer's instructions. Results were analyzed using a ChemiDoc XRS+ image analyzer (Bio-Rad). The intensity of chemiluminescence was measured using Quantity One software (Bio-Rad).

## RESULTS

**PP2 Inhibits SFK Activity in M Phase**—To synchronize cells in M phase, cells were arrested at the  $G_2$ /M boundary by treatment with the Cdk1 inhibitor RO-3306 and released into fresh medium. Microscopic analysis showed that cells progressed into M phase after release from  $G_2$  arrest and mostly completed M phase within 75 min (Fig. 1A). To examine the effect of inhibitors on SFK activity, M phase cells treated with inhibitors were collected by mitotic shake-off. Western blot analysis using anti-Src phospho-Tyr<sup>418</sup> antibody, which recognizes the autophosphorylation of SFKs, showed that the SFK inhibitor PP2 inhibited c-Src autophosphorylation (Fig. 1B). The MEK inhibitor U0126 was used as a negative control and did not show any inhibition of the autophosphorylation of SFKs, whereas phosphorylation of ERK1/2 by MEK was inhibited (Fig. 1B). Blotting with anti-phosphotyrosine antibody showed that the intensities of some bands specific to M phase were decreased upon treatment with PP2 (Fig. 1C), suggesting that Src signaling in M phase is suppressed by PP2 treatment.

To exclude the possibility that the inhibition of Src signaling would be the result of difference in mitotic stages, cells were released from  $G_2$  arrest with or without inhibitors and morphologically analyzed for chromosomes. Microscopic analysis showed that cells were in prophase or prometaphase, and treatment with PP2 or U0126 had no or only minor effects on cell cycle progression in these stages (Fig. 1D), confirming that the cells used for Western blot analysis were in similar stages of M phase.

We also examined the effect of the SFK inhibitor SU6656, which was originally identified as a potent and specific SFK inhibitor (47). Surprisingly, Western blot analysis using anti-phospho-Aurora A/B/C antibody revealed that SU6656 inhibited Aurora kinase activities in addition to SFKs (Fig. 1E). Importantly, PP2 did not show any inhibition of autophosphorylation of Aurora kinases (see Fig. 3D), suggesting that the target specificity of PP2 is higher than that of SU6656 in M phase cells. Thus, we decided to use PP2 for inhibition of SFKs in this study.

We next examined the localization of c-Src in M phase cells and found that c-Src was localized close to the spindle and spindle poles and that this localization was not inhibited by treatment with PP2 (Fig. 2, A and B). Immunofluorescence staining with anti-Src phospho-Tyr<sup>418</sup> antibody showed that

this antibody recognized inducibly expressed c-Src unless cells were treated with PP2 (Fig. 2, C and D), indicating that the kinase activity of c-Src was inhibited upon PP2 treatment. These results suggest that c-Src localization close to the mitotic spindle and spindle poles is independent of Src activity.

**Src Regulates Bipolar Spindle Formation**—To examine the role of Src signaling in spindle formation, HeLa S3 cells were arrested at late  $G_2$  phase by RO-3306 treatment (Fig. 1A) and released into fresh medium for 30 min in the presence of PP2 and/or the Aurora kinase inhibitor ZM447439. In control M phase cells, ~90 and 60% of the cells showed a bipolar spindle and aligned chromosomes at the cell equator, respectively (Fig. 3, A and B, *None*), suggesting that these M phase cells progressed into late prometaphase or metaphase. In this stage, we could not observe any significant effects of treatment with PP2 alone on spindle formation (Fig. 3, A and C). Intriguingly, treatment with PP2 plus ZM447439 revealed that the number of cells showing aberrant spindle formation was significantly increased (Fig. 3, A and C). The aberrations included monopolar spindles and misoriented bipolar spindles (Fig. 3A, *arrows*), in which the axis of spindle orientation was tilted to the surface of the culture dish (see Fig. 5) (48).

ZM447439 treatment strongly inhibited autophosphorylation of Aurora B at Thr<sup>232</sup> and phosphorylation of histone H3 at Ser<sup>10</sup> compared with autophosphorylation of Aurora A at Thr<sup>288</sup> (Fig. 3, D and E). In line with previous observations (49), chromosome alignment at the spindle equator was considerably disrupted by ZM447439 (Fig. 3B), although spindle formation was only partially affected (Fig. 3A). These results suggest that cells are arrested at a prometaphase-like stage upon treatment with ZM447439. We can assume that PP2 may inhibit spindle formation in prometaphase. It is of interest to note that the spindle is formed by at least two redundant pathways, the chromosome-mediated and centrosome-mediated pathways (3), and that chromosome-mediated spindle formation is predominantly inhibited by ZM447439 (10). PP2 treatment alone was incapable of inhibiting spindle formation in late prometaphase (Fig. 3C). We thus hypothesized that Src inhibition by treatment with PP2 may preferentially affect centrosome-mediated spindle formation in prophase and early prometaphase, which could be compensated by the other pathways in late prometaphase.

To ascertain the potential involvement of SFKs in the regulation of spindle formation, cells inducibly overexpressing c-Src were released into M phase in the presence of PP2 and/or ZM447439. We then examined the morphology of spindles and counted the number of M phase cells with a properly oriented bipolar spindle. In the presence of ZM447439, the number of properly oriented bipolar spindles was significantly increased following inducible c-Src overexpression (Fig. 4A, compare ZM447439 + *Dox* with ZM447439), and the increase was inhibited by PP2 treatment (Fig. 4A, ZM447439 + *Dox* + PP2). These results suggest that c-Src is involved in the formation of the mitotic spindle.

Interestingly, upon treatment with ZM447439, aster formation was severely inhibited in SYF cells, which harbor triple knock-out mutations of c-Src, c-Yes, and Fyn (Fig. 4B). Reintroduction of c-Src into SYF cells significantly restored aster

## Src Signaling Promotes Spindle Formation

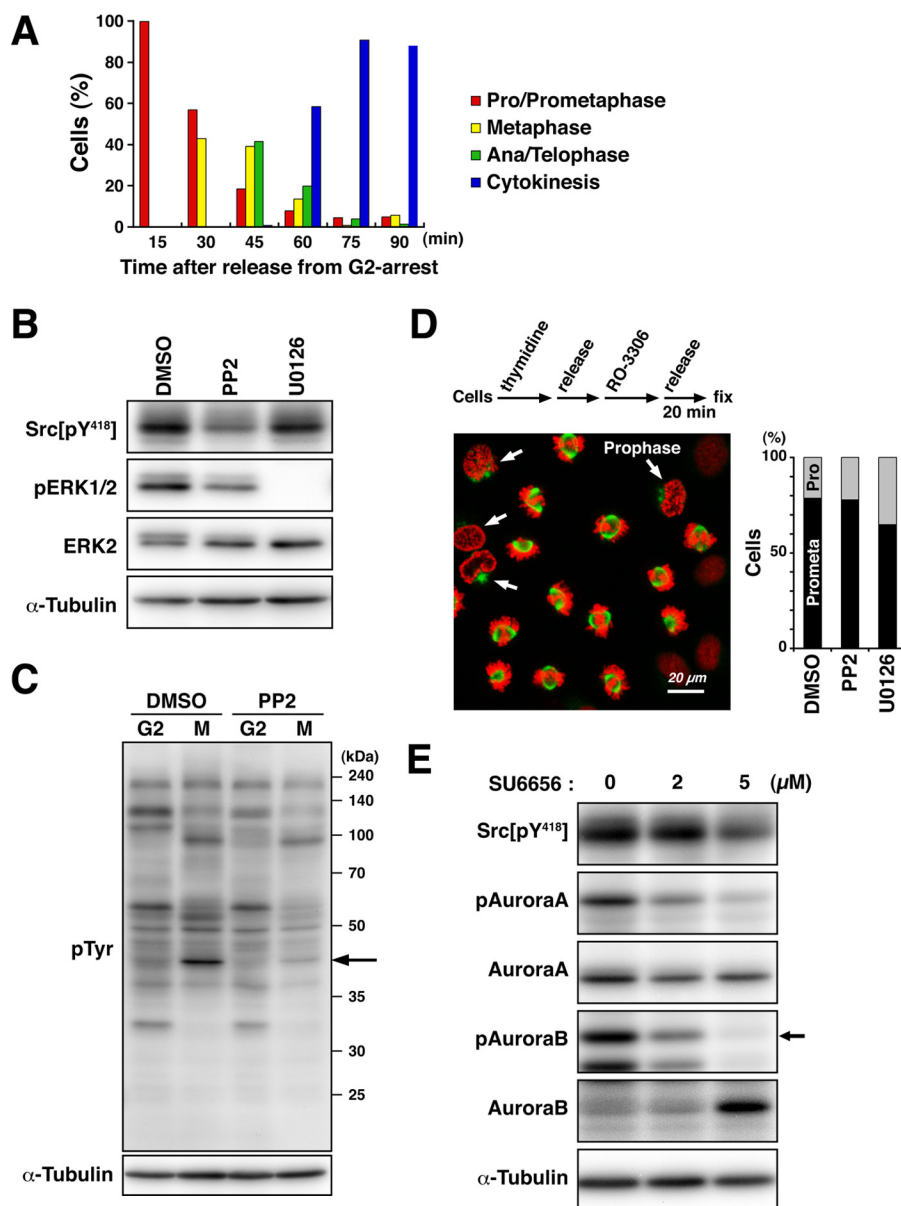


**FIGURE 1. PP2 inhibits Src activity in M phase.** *A*, HeLa S3 cells were arrested at late G<sub>2</sub> phase by treatment with 10 μM RO-3306 for 20 h. Subsequently, cells were washed with PBS supplemented with Ca<sup>2+</sup> and Mg<sup>2+</sup>, released into fresh medium, and fixed at the indicated time points. Fixed cells were stained for α-tubulin and DNA, and each mitotic step in M phase was quantified. *B* and *C*, HeLa S3 cells incubated with 4 mM thymidine were released for 5 h and then treated with 9 μM RO-3306 for 10 h to trap cells at late G<sub>2</sub> phase. Cells were treated with dimethyl sulfoxide (DMSO), 10 μM PP2, or 40 μM U0126 from the last 1 h of incubation with RO-3306, washed free of RO-3306, and then incubated for an additional 20 min in the continued presence of dimethyl sulfoxide, PP2, or U0126. Mitotic cells were collected by mitotic shake-off. Whole cell lysates were subjected to Western blotting, probed with anti-Src phospho-Tyr<sup>418</sup>, anti-phospho-ERK1/2, anti-ERK2, and anti-α-tubulin (loading control) antibodies (*B*) and anti-phosphotyrosine and anti-α-tubulin (loading control) antibodies (*C*). The arrow indicates the position of phosphorylated ERK2. *D*, HeLa S3 cells were synchronized at G<sub>2</sub> phase and treated with dimethyl sulfoxide, 10 μM PP2, or 40 μM U0126 as described for *B* and *C*. Cells were then fixed in PTEMF buffer and stained for α-tubulin (green) and DNA (red). Arrows indicate cells in prophase. Scale bar = 20 μm. M phase cells were dissected into prophase (Pro) and prometaphase (Prometa) cells, and the percentages of cells at each step in M phase cells were plotted (*n* > 588). *E*, HeLa S3 cells synchronized at late G<sub>2</sub> phase as described for *B* were released into fresh medium containing SU6656 at the indicated concentrations. Mitotic cells were collected by mitotic shake-off. Whole cell lysates were subjected to Western blotting and probed with anti-Src phospho-Tyr<sup>418</sup>, anti-phospho-Aurora A/B/C, anti-Aurora A, anti-Aurora B, and anti-α-tubulin (loading control) antibodies. The arrow indicates phosphorylated Aurora B.

formation (Fig. 4B). Furthermore, without ZM447439 treatment, we examined the effect of c-Src on microtubule regrowth from cold-induced depolymerization of microtubules. SYF and SYF/c-Src cells were incubated on ice for 4 h to completely depolymerize microtubules (44, 50, 51) and then returned to 37 °C for 90 s. Reintroduction of c-Src into SYF cells promoted aster formation from centrosomes after return to 37 °C (Fig. 4C). These results suggest that the kinase activities of SFKs may promote aster formation on centrosomes.

*Src Regulates Spindle Orientation in Early Prometaphase—* Although the centrosome is dispensable for spindle formation (1), spindles are frequently misoriented by centrosome ablation due to loss of astral microtubules (2). To examine the role of SFKs in centrosome-mediated spindle formation, cells were examined for spindle orientation in early prometaphase. After HeLa S3 cells arrested at late G<sub>2</sub> phase were released into fresh medium containing nocodazole for 30 min, a subsequent 15-min release from the nocodazole arrest ensured careful

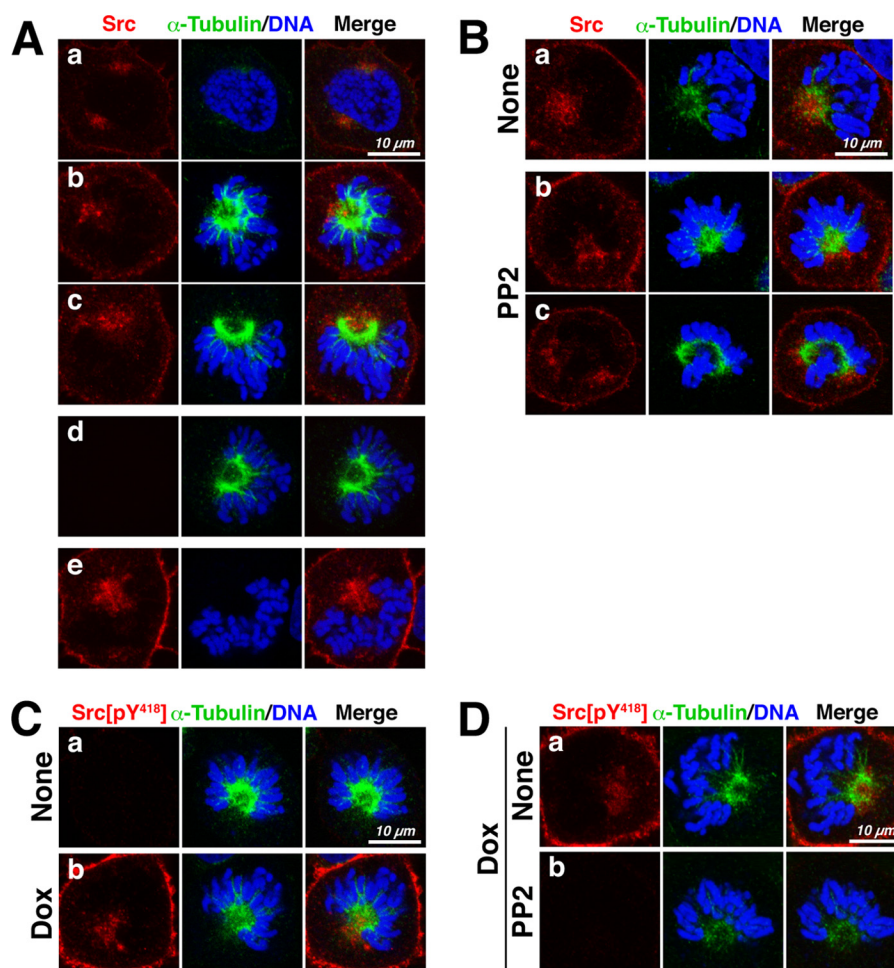


FIGURE 2. **Src localizes to or close to mitotic spindles.** *A*, HeLa S3 cells inducibly overexpressing c-Src were fixed in 4% paraformaldehyde for 3 min and extracted with 0.5% Triton X-100 for 5 min at room temperature, followed by further fixation in 4% paraformaldehyde for 15 min. Fixed cells were stained for c-Src (red),  $\alpha$ -tubulin (green), and DNA (blue) (panels a–c). Cells were stained with either anti- $\alpha$ -tubulin antibody (panel d) or anti-Src antibody (panel e) alone. *B*, HeLa S3 cells expressing c-Src were treated with 20  $\mu$ M PP2 and then fixed and stained for c-Src,  $\alpha$ -tubulin, and DNA as described for *A*. *C*, c-Src-inducible HeLa S3 cells were treated with or without 1  $\mu$ g/ml doxycycline (Dox) and then fixed as described for *A*. Fixed cells were stained for anti-Src phospho-Tyr<sup>418</sup> antibody (red),  $\alpha$ -tubulin (green), and DNA (blue). *D*, HeLa S3 cells overexpressing c-Src were treated with 20  $\mu$ M PP2 for 3 h, fixed, and stained as described for *C*. Scale bars = 10  $\mu$ m.

scrutinization of spindle formation in early prometaphase. Three-dimensional analyses showed that two spindle poles formed in a mitotic spindle were positioned on the same focal plane in control mitotic cells (Fig. 5*A*, None,  $Z=24$ , arrows), indicating that the axis of spindle orientation was parallel to the surface of culture dish. Intriguingly, Src inhibition by PP2 treatment of mitotic cells showed that both spindle poles in a mitotic spindle were often positioned on different focal planes (Fig. 5*A*, PP2,  $Z=7$  and  $Z=37$ , arrows), indicating that the axis of spindle orientation was tilted to the surface of the culture dish, *i.e.* the spindle was misoriented. The number of cells showing spindle misorientation was significantly increased in PP2-treated cells irrespective of Aurora kinase inhibition by ZM447439 treatment. These results suggest that SFKs may regulate spindle orientation through centrosome-mediated spindle formation in early prometaphase.

SYF, SYF/c-Src, and SYF/Fyn cells were released for 15 min from nocodazole arrest and compared for spindle orientation. The number of cells showing spindle misorientation was increased in SYF cells compared with HeLa S3 cells (compare Fig. 6*B* with Fig. 5*B*), suggesting that the combined deficiencies

of c-Src, c-Yes, and Fyn in SYF cells augment spindle misorientation. Reintroduction of c-Src in SYF cells decreased the number of cells with a misoriented spindle, but reintroduction of Fyn in SYF cells was not as efficient in restoring proper spindle orientation compared with c-Src (Fig. 6*B*). These results suggest that c-Src is preferentially involved in proper spindle orientation in early prometaphase. In these experiments, we also quantified the percentages of cells that progressed into anaphase and found that the number of anaphase cells with properly oriented spindles was increased in SYF/c-Src cells compared with SYF cells (Fig. 6*C*), suggesting that the role of c-Src in spindle formation is critical for mitotic progression.

## DISCUSSION

In this study, we have shown that mitotic activation of c-Src is critically involved in astral microtubule formation that influences spindle orientation in early prometaphase and mitotic progression.

**Src Localization around Spindle Poles**—We have shown that c-Src is localized close to the spindle and spindle poles. Because centrosomes accelerate entry into mitosis by increasing the

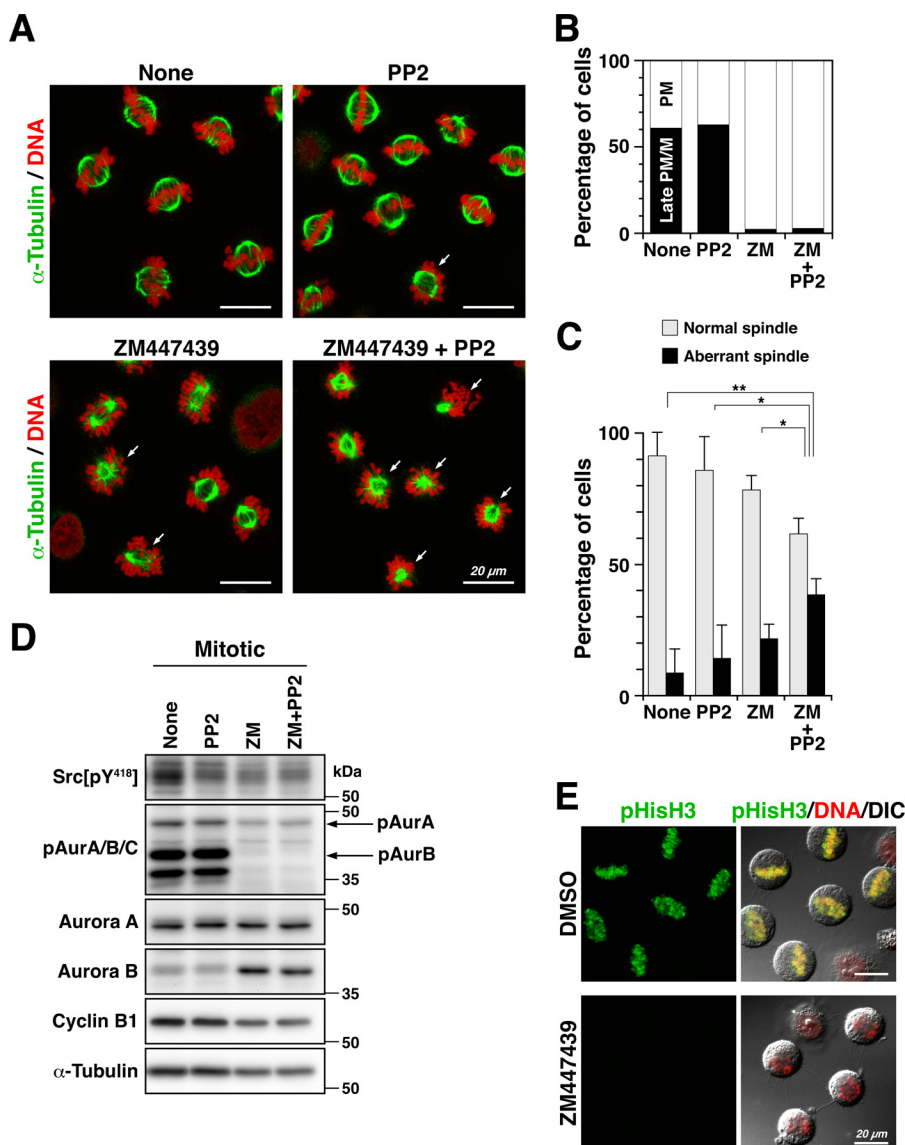


**FIGURE 3. Spindle formation is disrupted by simultaneous inhibition of SFKs and Aurora B.** A–C, HeLa S3 cells arrested at late G<sub>2</sub> phase with RO-3306 were released into fresh medium containing 10  $\mu$ M ZM447439 (ZM), 20  $\mu$ M PP2, or 10  $\mu$ M ZM447439 plus 20  $\mu$ M PP2 for 30 min. Cells were then fixed in PTEMF buffer for 20 min at 37 °C. A, fixed cells were stained for  $\alpha$ -tubulin and DNA. Arrows indicate cells exhibiting aberrant spindles, including misorientation and monopolar spindle formation. Scale bars = 20  $\mu$ m. B, M phase cells were dissected into early prometaphase (PM, open bar) and late prometaphase/metaphase (Late PM/M, closed bar) cells, and the percentages of cells at each step in M phase cells were plotted ( $n > 899$ ). C, M phase cells were morphologically examined for spindles. The percentages of cells with a properly oriented bipolar spindle or an aberrant spindle, including misoriented bipolar spindles and monopolar spindles in M phase cells ( $n > 1255$ ), are presented as means  $\pm$  S.D. from three independent experiments. Asterisks indicate significant differences (\*,  $p < 0.05$ ; \*\*,  $p < 0.01$ ) in Student's two-tailed t test.  $p$  values are 0.0078 (None versus ZM + PP2), 0.037 (PP2 versus ZM + PP2), 0.020 (ZM versus ZM + PP2), and 0.091 (None versus ZM). D, G<sub>2</sub>-arrested HeLa S3 cells were released into fresh medium with or without 10  $\mu$ M ZM447439 and 20  $\mu$ M PP2. At 30 min after release, whole cell lysates were prepared and subjected to Western blotting using anti-Src phospho-Tyr<sup>418</sup>, anti-phospho-Aurora A/B/C (pAurA/B/C), anti-Aurora A, anti-Aurora B, anti-cyclin B<sub>1</sub>, and anti- $\alpha$ -tubulin (loading control) antibodies. E, G<sub>2</sub>-arrested cells were released into fresh medium with or without 10  $\mu$ M ZM447439. Cells fixed in paraformaldehyde were permeabilized with methanol and then stained for phosphohistone H3 at Ser<sup>10</sup> (pHisH3) and DNA. DIC, differential interference contrast; DMSO, dimethyl sulfoxide. Scale bars = 20  $\mu$ m.

local concentration of Cdk1/cyclin B (52), c-Src localized around centrosomes may be preferentially activated by Cdk1. A previous report showed that a non-myristoylated mutant of c-Src associates with the mitotic spindles and spindle poles in NIH 3T3-derived cells (25). Approximately 16% of newly synthesized Src is not myristoylated and fails to associate with membranes (53). Besides the myristoyl residue, the basic cluster at the N terminus of c-Src has been reported to play a role in membrane attachment (54). Phosphorylation of the site close to the cluster can interfere with the electrostatic interactions that anchor c-Src to the lipid bilayer (55), resulting in inhibition of

membrane attachment. It is interesting to note that Cdk1 phosphorylation sites were reported in the N-terminal unique domain (19–22). We can assume that, upon mitotic entry, non-myristoylated c-Src associates with the centrosomes and is phosphorylated by Cdk1 around the centrosomes. Phosphorylation in the N-terminal region might lead to masking of the basic cluster and prevent c-Src from returning to the plasma membrane, resulting in further accumulation of c-Src around centrosomes and activation.

**Roles of SFKs in Regulation of M Phase**—It was reported previously that G<sub>2</sub>-M transition was blocked when SFKs were

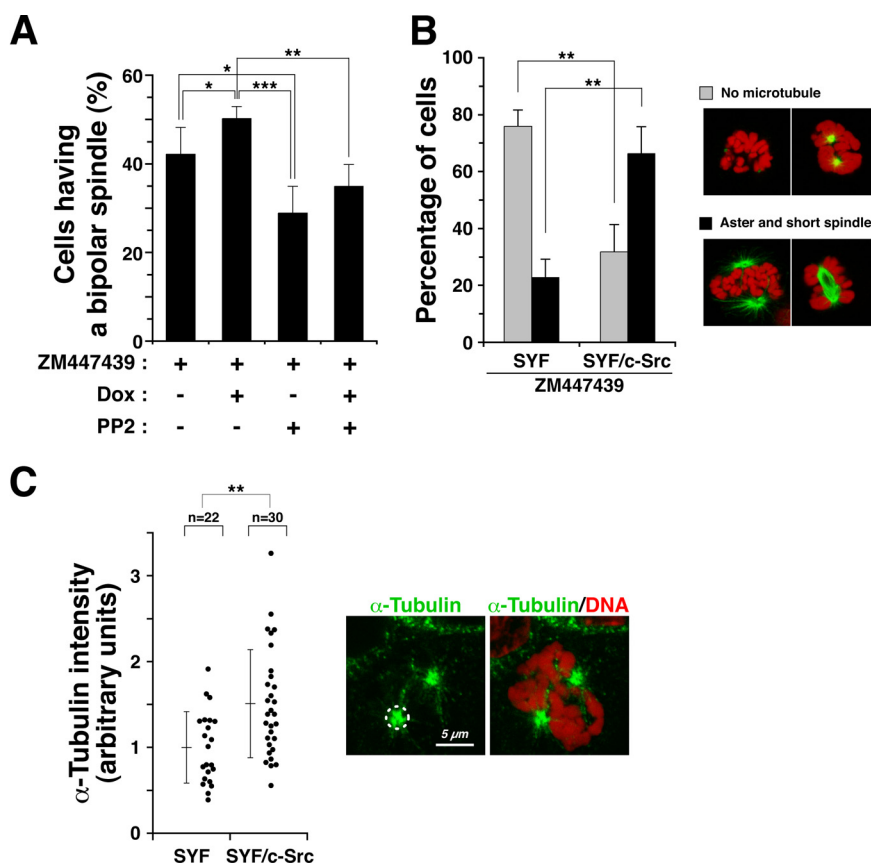


**FIGURE 4. c-Src is involved in bipolar spindle formation.** *A*, c-Src-inducible cells were cultured in the presence of 1  $\mu$ g/ml doxycycline (Dox) for 2 days to induce c-Src overexpression, and during the last 20 h of induction, cells were treated with 9  $\mu$ M RO-3306 to arrest cells at late G<sub>2</sub> phase. G<sub>2</sub>-arrested cells were released into medium containing 20  $\mu$ M PP2, 10  $\mu$ M ZM447439, or 20  $\mu$ M PP2 plus 10  $\mu$ M ZM447439 for 30 min and fixed in 4% paraformaldehyde. The percentages of M phase cells with a properly oriented bipolar spindle ( $n > 1115$ ) are presented as means  $\pm$  S.D. from three independent experiments. Asterisks indicate significant differences (\*,  $p < 0.05$ ; \*\*,  $p < 0.01$ ; \*\*\*,  $p < 0.001$ ) in Student's two-tailed *t* test. *p* values are 0.047 (ZM versus ZM + Dox), 0.019 (ZM versus ZM + PP2), 0.00057 (ZM + Dox versus ZM + PP2), and 0.0014 (ZM + Dox versus ZM + Dox + PP2). *B*, SYF and SYF/c-Src cells were treated with 8  $\mu$ M RO-3306 for 20 h, washed free of RO-3306, and then incubated with 0.1  $\mu$ g/ml nocodazole and 10  $\mu$ M ZM447439 for 30 min at 37  $^{\circ}$ C. Cells were washed free of nocodazole and incubated for an additional 15 min in the continued presence of 10  $\mu$ M ZM447439. Cells were fixed in PTEMF buffer for 20 min and stained for  $\alpha$ -tubulin (green) and DNA (red). Mitotic cells were examined for microtubule polymerization and classified into two categories as follows: no microtubules (gray bars) and aster and short spindles (black bars). The cells in these categories were counted. The data (expressed as percentages of the mitotic cells) are means  $\pm$  S.D. from three independent experiments ( $n > 271$ ). Asterisks indicate significant differences (\*\*,  $p < 0.01$ ) in Student's two-tailed *t* test. *p* values are 0.0021 (SYF, No microtubule versus SYF/c-Src, No microtubule), 0.0025 (SYF, Aster and short spindle versus SYF/c-Src, Aster and short spindle). *C*, SYF and SYF/c-Src cells were incubated on ice for 4 h to completely depolymerize microtubules and fixed at 90 s after return to 37  $^{\circ}$ C. Fixed cells were stained for  $\alpha$ -tubulin (green) and DNA (red), and the integrated fluorescence intensity of  $\alpha$ -tubulin staining was measured in a circle centered on the centrosome with a radius of 1.5  $\mu$ m, as shown with the dashed line. The plot represents the relative intensities to the mean intensity of SYF cells ( $n > 22$ ). Error bars represent means  $\pm$  S.D. from three independent experiments. The asterisk indicates significant differences (\*\*,  $p < 0.01$ ) in Student's two-tailed *t* test. *p* values are 0.0018 (SYF versus SYF/c-Src).

inhibited by microinjection of anti-Src antibody (16). We also reported that lengthy treatment with PP2 prevented cells from entering into M phase (15). However, short exposure of cells to PP2 did not prevent cells from mitotic entry as shown in Fig. 1*D*. These results suggest that the PP2 treatment performed in this study was not enough to completely inhibit the activities of SFKs. Indeed, autophosphorylation of Src, which can be detected with anti-Src phospho-Tyr<sup>418</sup> antibody, was only partially inhibited by treatment with PP2 (Figs. 1*B* and 3*D*). Consistently, spindle orientation was only partially inhibited. Because lengthy exposure to PP2 prevents cells from mitotic entry, this would not have been suitable in this study to examine the role of SFKs in M phase.

Accordingly, we used SYF cells to examine the effect of lack of SFK kinase activity. Although SYF cells harbor triple knockout mutations of c-Src, c-Yes, and Fyn, SYF cells were reported to still express two SFK members, Hck and c-Fgr (56), and coexpression of multiple SYF members is suggested to play a redun-

dant role. This may be the reason why SYF cells can divide. However, we found defects in mitotic spindle orientation in SYF cells. In particular, aster mitotic spindle formation in SYF cells was blocked by Aurora kinase inhibition, and c-Src reintroduction rescued the blockade of aster spindle formation by Aurora kinase inhibition (Fig. 4*B*). Moreover, Src inhibition by PP2 in HeLa cells induced spindle misorientation irrespective of Aurora kinase inhibition (Fig. 5). Thus, we conclude that c-Src plays a role in aster spindle formation that contributes to spindle orientation.

**Mitotic Spindle Formation Involving Src Signaling in Early Prometaphase**—Aurora A has been reported to play a key role in centrosome-mediated spindle formation (57, 58). We tested whether c-Src overexpression increases mitotic autophosphorylation of Aurora A at Thr<sup>288</sup> in HeLa cells. However, we did not find any differences in the autophosphorylation levels of Aurora A in control expression and inducible overexpression of c-Src (supplemental Fig. S2). Similar results were seen in SYF

## Src Signaling Promotes Spindle Formation

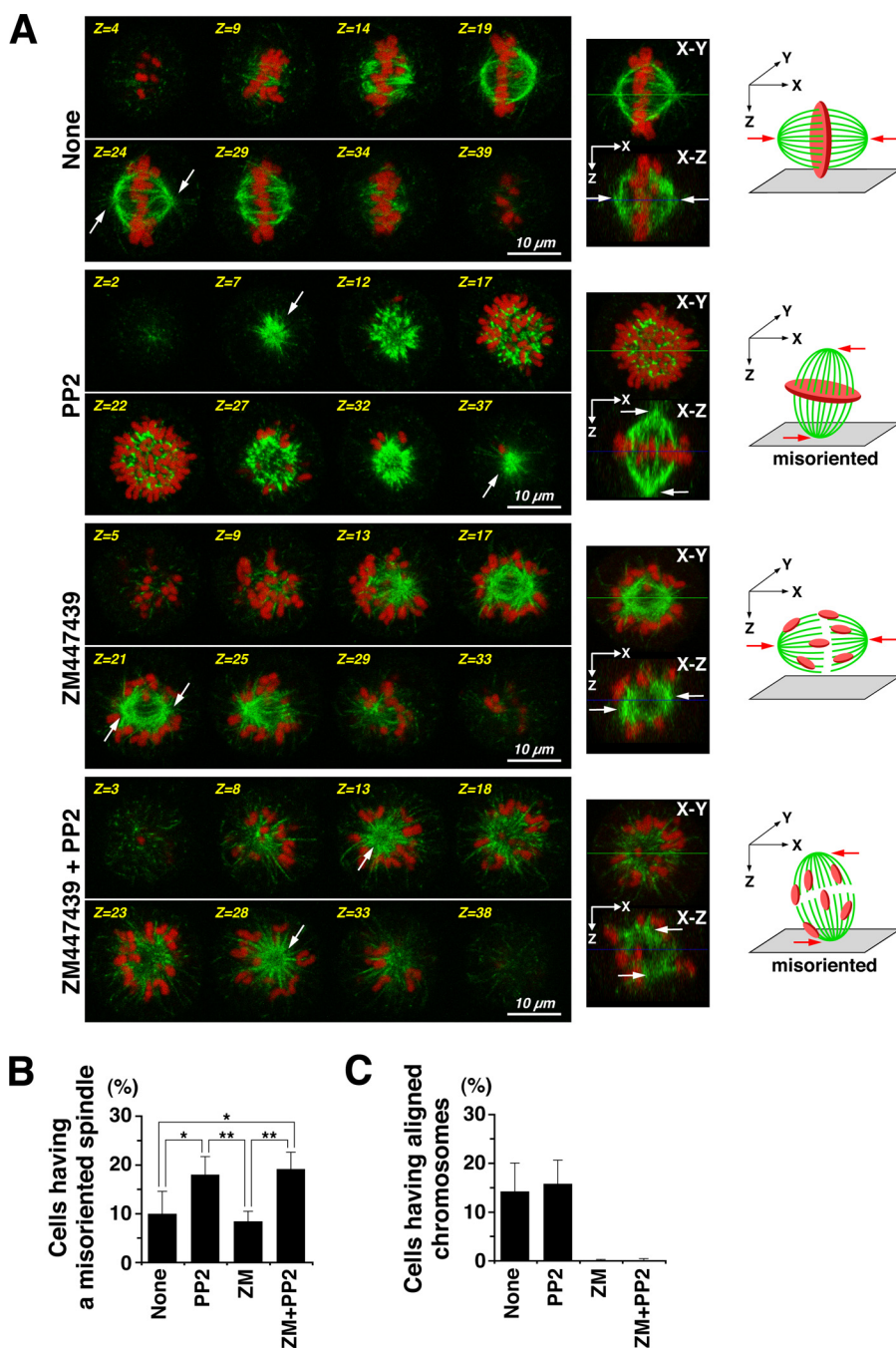


**FIGURE 5. SFKs regulate spindle orientation in early prometaphase.** HeLa S3 cells arrested at late G<sub>2</sub> phase were released into medium containing nocodazole for 30 min. The nocodazole-arrested cells were then released into nocodazole-free fresh medium for only 15 min to proceed into early prometaphase. During the nocodazole treatment and the release from nocodazole, cells were treated with 10  $\mu$ M ZM447439 (ZM), 20  $\mu$ M PP2, or 10  $\mu$ M ZM447439 plus 20  $\mu$ M PP2. Cells were fixed with paraformaldehyde and stained for  $\alpha$ -tubulin and DNA. *A*, *left*, Z-stack images of eight focal planes (1.6~2.25  $\mu$ m apart). *Middle*, the images of the middle focal planes (X-Y) and the X-Z projections from the Z-stack images of 40~44 focal planes (0.35~0.45  $\mu$ m apart). *Right*, schematic diagrams showing spindle orientation and misorientation with aligned or scattered chromosomes. Scale bars = 10  $\mu$ m. Arrows indicate the positions of spindle poles. *B*, the percentages of M phase cells with a misoriented spindle ( $n > 884$ ) are presented as means  $\pm$  S.D. from four independent experiments. Asterisks indicate significant differences (\*,  $p < 0.05$ ; \*\*,  $p < 0.01$ ) in Student's two-tailed *t* test. *p* values are 0.032 (None versus PP2), 0.017 (None versus ZM + PP2), 0.0034 (PP2 versus ZM), and 0.0014 (ZM versus ZM + PP2). *C*, the percentages of M phase cells with aligned chromosomes ( $n > 865$ ) are presented as means  $\pm$  S.D. from four independent experiments.

and SYF/c-Src cells. In addition, we did not detect an effect of c-Src overexpression on the centrosomal localization of Aurora A (supplemental Fig. S2). These results suggest that c-Src may act independently of Aurora A to form centrosome-mediated mitotic spindles.

We reported previously that Src kinase activity during early mitosis mediates MEK/ERK activation for abscission in cytoki-

nesis (15). We have shown here that the band intensity of phosphorylated ERK was decreased upon treatment with PP2 and completely lost upon U0126 treatment in prometaphase cells (Fig. 1B). Given that the phosphotyrosine residue in the activation loop of ERK is indicative of ERK activation and is recognized by anti-phospho-ERK and anti-phosphotyrosine antibodies (Fig. 1, B and C), these results suggest that ERK is



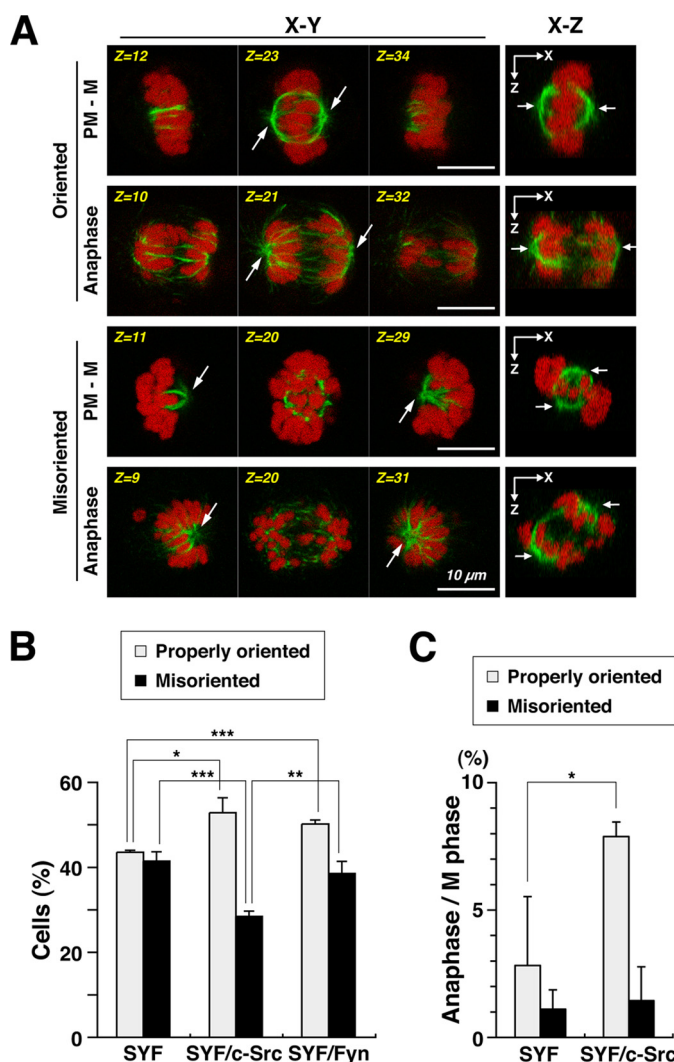


**FIGURE 6. Triple knock-out mutations of c-Src, c-Yes, and Fyn result in spindle misorientation.** SYF, SYF/c-Src, and SYF/Fyn cells arrested at late G<sub>2</sub> phase were released into medium containing nocodazole for 30 min. The nocodazole-arrested cells were then released into nocodazole-free fresh medium for 15 min. Cells were fixed with paraformaldehyde and stained for  $\alpha$ -tubulin and DNA. *A, left*, Z-stack images of three focal planes (3.15–4.4  $\mu$ m apart). *Right*, the X-Z projections from the Z-stack images of 40–44 focal planes (0.35–0.4  $\mu$ m apart). Arrows indicate the positions of spindle poles. PM - M, prometaphase to metaphase. Scale bars = 10  $\mu$ m. *B*, the percentages of prometaphase, metaphase, and anaphase cells with a properly oriented spindle or a misoriented spindle in M phase ( $n > 608$ ) are presented as means  $\pm$  S.D. from three independent experiments. Asterisks indicate significant differences (\*,  $p < 0.05$ ; \*\*,  $p < 0.01$ ; \*\*\*,  $p < 0.001$ ) in Student's two-tailed *t* test. *p* values are 0.039 (SYF, Properly oriented versus SYF/c-Src, Properly oriented), 0.00026 (SYF, Properly oriented versus SYF/Fyn, Properly oriented), 0.00067 (SYF, Misoriented versus SYF/c-Src, Misoriented), and 0.0040 (SYF/c-Src, Misoriented versus SYF/Fyn, Misoriented). *C*, the percentages of anaphase cells with a properly oriented spindle or a misoriented spindle in M phase cells ( $n > 662$ ) are presented as means  $\pm$  S.D. from three independent experiments. The Asterisk indicates significant difference (\*,  $p < 0.05$ ) in Student's two-tailed *t* test. *p* values are 0.034 (SYF, Properly oriented versus (SYF/c-Src, Properly oriented).

activated downstream of SFKs upon mitotic entry in a manner dependent on MEK activities.

ERK localizes to the mitotic spindle (59), and nocodazole treatment does not activate ERK (60–62). MEK/ERK signaling plays a role in regulation of the mitotic spindle (59, 63). In addition, c-Src associates with the mitotic spindle (25). These results raise the intriguing possibility that the spindle and spin-

dle poles serve as a signaling platform for Src/MEK/ERK activation. It is interesting to speculate that, upon mitotic entry, SFKs may be activated by Cdk1 on centrosomes and lead to activation of the MEK/ERK signaling cascade on the centrosomes and newly polymerizing microtubules, promoting astral microtubule formation. If Src signaling is inhibited, the spindle is misoriented due to deregulation of centrosome-mediated astral microtubule formation. Further investigation will be required to clarify the involvement of MEK/ERK signaling in Src-regulated spindle orientation.

Microtubule assembly from centrosomes is involved in the formation of astral microtubules, which play roles in regulation of the position of spindles and spindle orientation through interactions between astral microtubules and the cell cortex (48, 64). Mitotic spindle orientation has been proposed to control cell fate choices, tissue architecture, and tissue morphogenesis (65). Considering our previous result that overexpression of Chk, a negative regulator of SFKs, induces insufficient formation of mitotic spindles and aberrant chromosome movement, leading to multinucleation (28), the findings presented here provide further evidence that SFK kinase activity plays an important role in spindle organization through regulation of centrosome-mediated spindle formation, in particular astral microtubule formation. It is now of interest to identify substrate molecules downstream of Src signaling on the mitotic spindle, which will help us gain a further understanding of centrosome-mediated spindle formation in early prometaphase.

*Acknowledgments*—We are indebted to Dr. Donald J. Fujita (University of Calgary) and Dr. Stéphane A. Laporte (McGill University) for valuable plasmids.

## REFERENCES

- Heald, R., Tournebise, R., Blank, T., Sandaltzopoulos, R., Becker, P., Hyman, A., and Karsenti, E. (1996) Self-organization of microtubules into bipolar spindles around artificial chromosomes in *Xenopus* egg extracts. *Nature* **382**, 420–425
- Khodjakov, A., Cole, R. W., Oakley, B. R., and Rieder, C. L. (2000) Centrosome-independent mitotic spindle formation in vertebrates. *Curr. Biol.* **10**, 59–67
- Gadde, S., and Heald, R. (2004) Mechanisms and molecules of the mitotic spindle. *Curr. Biol.* **14**, R797–R805
- Bettencourt-Dias, M., and Glover, D. M. (2007) Centrosome biogenesis and function: centrosomics brings new understanding. *Nat. Rev. Mol. Cell Biol.* **8**, 451–463
- Hannak, E., Kirkham, M., Hyman, A. A., and Oegema, K. (2001) Aurora A kinase is required for centrosome maturation in *Caenorhabditis elegans*. *J. Cell Biol.* **155**, 1109–1116
- Berdnik, D., and Knoblich, J. A. (2002) *Drosophila* Aurora A is required for centrosome maturation and actin-dependent asymmetric protein localization during mitosis. *Curr. Biol.* **12**, 640–647
- Terada, Y., Uetake, Y., and Kuriyama, R. (2003) Interaction of Aurora A and centrosomin at the microtubule-nucleating site in *Drosophila* and mammalian cells. *J. Cell Biol.* **162**, 757–763
- Carmena, M., Ruchaud, S., and Earnshaw, W. C. (2009) Making the Auroras glow: regulation of Aurora A and B kinase function by interacting proteins. *Curr. Opin. Cell Biol.* **21**, 796–805
- Ruchaud, S., Carmena, M., and Earnshaw, W. C. (2007) Chromosomal passengers: conducting cell division. *Nat. Rev. Mol. Cell Biol.* **8**, 798–812
- Gadea, B. B., and Ruderman, J. V. (2005) Aurora kinase inhibitor ZM447439 blocks chromosome-induced spindle assembly, the comple-

## Src Signaling Promotes Spindle Formation

- tion of chromosome condensation, and the establishment of the spindle integrity checkpoint in *Xenopus* egg extracts. *Mol. Biol. Cell* **16**, 1305–1318
11. Brown, M. T., and Cooper, J. A. (1996) Regulation, substrates, and functions of Src. *Biochim. Biophys. Acta* **1287**, 121–149
  12. Thomas, S. M., and Brugge, J. S. (1997) Cellular functions regulated by Src family kinases. *Annu. Rev. Cell Dev. Biol.* **13**, 513–609
  13. Moasser, M. M., Srethapakdi, M., Sachar, K. S., Kraker, A. J., and Rosen, N. (1999) Inhibition of Src kinases by a selective tyrosine kinase inhibitor causes mitotic arrest. *Cancer Res.* **59**, 6145–6152
  14. Ng, M. M., Chang, F., and Burgess, D. R. (2005) Movement of membrane domains and requirement of membrane signaling molecules for cytokinesis. *Dev. Cell* **9**, 781–790
  15. Kasahara, K., Nakayama, Y., Nakazato, Y., Ikeda, K., Kuga, T., and Yamaguchi, N. (2007) Src signaling regulates completion of abscission in cytokinesis through ERK/MAPK activation at the midbody. *J. Biol. Chem.* **282**, 5327–5339
  16. Roche, S., Fumagalli, S., and Courtneidge, S. A. (1995) Requirement for Src family protein-tyrosine kinases in G<sub>2</sub> for fibroblast cell division. *Science* **269**, 1567–1569
  17. Tominaga, T., Sahai, E., Chardin, P., McCormick, F., Courtneidge, S. A., and Alberts, A. S. (2000) Diaphanous-related formins bridge Rho GTPase and Src tyrosine kinase signaling. *Mol. Cell* **5**, 13–25
  18. Hanke, J. H., Gardner, J. P., Dow, R. L., Changelian, P. S., Brissette, W. H., Weringer, E. J., Pollok, B. A., and Connelly, P. A. (1996) Discovery of a novel, potent, and Src family-selective tyrosine kinase inhibitor. Study of Lck- and FynT-dependent T cell activation. *J. Biol. Chem.* **271**, 695–701
  19. Chackalaparampil, I., and Shalloway, D. (1988) Altered phosphorylation and activation of pp60<sup>c-src</sup> during fibroblast mitosis. *Cell* **52**, 801–810
  20. Morgan, D. O., Kaplan, J. M., Bishop, J. M., and Varmus, H. E. (1989) Mitosis-specific phosphorylation of p60<sup>c-src</sup> by p34<sup>cdc2</sup>-associated protein kinase. *Cell* **57**, 775–786
  21. Zheng, X. M., and Shalloway, D. (2001) Two mechanisms activate PTP $\alpha$  during mitosis. *EMBO J.* **20**, 6037–6049
  22. Kesavan, K. P., Isaacson, C. C., Ashendel, C. L., Geahlen, R. L., and Harrison, M. L. (2002) Characterization of the *in vivo* sites of serine phosphorylation on Lck identifying serine 59 as a site of mitotic phosphorylation. *J. Biol. Chem.* **277**, 14666–14673
  23. Kuga, T., Nakayama, Y., Hoshino, M., Higashiyama, Y., Obata, Y., Matsuda, D., Kasahara, K., Fukumoto, Y., and Yamaguchi, N. (2007) Differential mitotic activation of endogenous c-Src, c-Yes, and Lyn in HeLa cells. *Arch. Biochem. Biophys.* **466**, 116–124
  24. McGinnis, L. K., Albertini, D. F., and Kinsey, W. H. (2007) Localized activation of Src family protein kinases in the mouse egg. *Dev. Biol.* **306**, 241–254
  25. David-Pfeuty, T., Bagrodia, S., and Shalloway, D. (1993) Differential localization patterns of myristoylated and non-myristoylated c-Src proteins in interphase and mitotic c-Src overexpressor cells. *J. Cell Sci.* **105**, 613–628
  26. Ley, S. C., Marsh, M., Bebbington, C. R., Proudfoot, K., and Jordan, P. (1994) Distinct intracellular localization of Lck and Fyn protein-tyrosine kinases in human T lymphocytes. *J. Cell Biol.* **125**, 639–649
  27. Talmor-Cohen, A., Tomashov-Matar, R., Tsai, W. B., Kinsey, W. H., and Shalgi, R. (2004) Fyn kinase-tubulin interaction during meiosis of rat eggs. *Reproduction* **128**, 387–393
  28. Yamaguchi, N., Nakayama, Y., Urakami, T., Suzuki, S., Nakamura, T., Suda, T., and Oku, N. (2001) Overexpression of the Csk homologous kinase (Chk tyrosine kinase) induces multinucleation: a possible role for chromosome-associated Chk in chromosome dynamics. *J. Cell Sci.* **114**, 1631–1641
  29. Fessart, D., Simaan, M., and Laporte, S. A. (2005) c-Src regulates clathrin adapter protein 2 interaction with  $\beta$ -arrestin and the angiotensin II type 1 receptor during clathrin-mediated internalization. *Mol. Endocrinol.* **19**, 491–503
  30. Nakayama, Y., Igarashi, A., Kikuchi, I., Obata, Y., Fukumoto, Y., and Yamaguchi, N. (2009) Bleomycin-induced over-replication involves sustained inhibition of mitotic entry through the ATM/ATR pathway. *Exp. Cell Res.* **315**, 2515–2528
  31. Bjorge, J. D., Bellagamba, C., Cheng, H. C., Tanaka, A., Wang, J. H., and Fujita, D. J. (1995) Characterization of two activated mutants of human pp60<sup>c-src</sup> that escape c-Src kinase regulation by distinct mechanisms. *J. Biol. Chem.* **270**, 24222–24228
  32. Klinghoffer, R. A., Sachsenmaier, C., Cooper, J. A., and Soriano, P. (1999) Src family kinases are required for integrin but not PDGFR signal transduction. *EMBO J.* **18**, 2459–2471
  33. Takahashi, A., Obata, Y., Fukumoto, Y., Nakayama, Y., Kasahara, K., Kuga, T., Higashiyama, Y., Saito, T., Yokoyama, K. K., and Yamaguchi, N. (2009) Nuclear localization of Src family tyrosine kinases is required for growth factor-induced euchromatinization. *Exp. Cell Res.* **315**, 1117–1141
  34. Fukumoto, Y., Obata, Y., Ishibashi, K., Tamura, N., Kikuchi, I., Aoyama, K., Hattori, Y., Tsuda, K., Nakayama, Y., and Yamaguchi, N. (2010) Cost-effective gene transfection by DNA compaction at pH 4.0 using acidified, long shelf-life polyethylenimine. *Cytotechnology* **62**, 73–82
  35. Kuga, T., Hoshino, M., Nakayama, Y., Kasahara, K., Ikeda, K., Obata, Y., Takahashi, A., Higashiyama, Y., Fukumoto, Y., and Yamaguchi, N. (2008) Role of Src family kinases in formation of the cortical actin cap at the dorsal cell surface. *Exp. Cell Res.* **314**, 2040–2054
  36. Kasahara, K., Nakayama, Y., Sato, I., Ikeda, K., Hoshino, M., Endo, T., and Yamaguchi, N. (2007) Role of Src family kinases in formation and trafficking of macropinosomes. *J. Cell. Physiol.* **211**, 220–232
  37. Kasahara, K., Nakayama, Y., Kihara, A., Matsuda, D., Ikeda, K., Kuga, T., Fukumoto, Y., Igarashi, Y., and Yamaguchi, N. (2007) Rapid trafficking of c-Src, a non-palmitoylated Src family kinase, between the plasma membrane and late endosomes/lysosomes. *Exp. Cell Res.* **313**, 2651–2666
  38. Sato, I., Obata, Y., Kasahara, K., Nakayama, Y., Fukumoto, Y., Yamasaki, T., Yokoyama, K. K., Saito, T., and Yamaguchi, N. (2009) Differential trafficking of Src, Lyn, Yes, and Fyn is specified by the state of palmitoylation in the SH4 domain. *J. Cell Sci.* **122**, 965–975
  39. Yamaguchi, N., and Fukuda, M. N. (1995) Golgi retention mechanism of  $\beta$ -1,4-galactosyltransferase. Membrane-spanning domain-dependent homodimerization and association with  $\alpha$ - and  $\beta$ -tubulins. *J. Biol. Chem.* **270**, 12170–12176
  40. Kasahara, K., Nakayama, Y., Ikeda, K., Fukushima, Y., Matsuda, D., Horimoto, S., and Yamaguchi, N. (2004) Trafficking of Lyn through the Golgi caveolin involves the charged residues on  $\alpha$ E and  $\alpha$ I helices in the kinase domain. *J. Cell Biol.* **165**, 641–652
  41. Nakayama, Y., and Yamaguchi, N. (2005) Multi-lobulation of the nucleus in prolonged S phase by nuclear expression of Chk tyrosine kinase. *Exp. Cell Res.* **304**, 570–581
  42. Ikeda, K., Nakayama, Y., Togashi, Y., Obata, Y., Kuga, T., Kasahara, K., Fukumoto, Y., and Yamaguchi, N. (2008) Nuclear localization of Lyn tyrosine kinase mediated by inhibition of its kinase activity. *Exp. Cell Res.* **314**, 3392–3404
  43. Obata, Y., Fukumoto, Y., Nakayama, Y., Kuga, T., Dohmae, N., and Yamaguchi, N. (2010) The Lyn kinase C-lobe mediates Golgi export of Lyn through conformation-dependent ACSL3 association. *J. Cell Sci.* **123**, 2649–2662
  44. Brinkley, B. R., and Cartwright, J. Jr. (1975) Cold-labile and cold-stable microtubules in the mitotic spindle of mammalian cells. *Ann. N.Y. Acad. Sci.* **253**, 428–439
  45. Nakayama, Y., Kawana, A., Igarashi, A., and Yamaguchi, N. (2006) Involvement of the N-terminal unique domain of Chk tyrosine kinase in Chk-induced tyrosine phosphorylation in the nucleus. *Exp. Cell Res.* **312**, 2252–2263
  46. Kikuchi, I., Nakayama, Y., Morinaga, T., Fukumoto, Y., and Yamaguchi, N. (2010) A decrease in cyclin B<sub>1</sub> levels leads to polyploidization in DNA damage-induced senescence. *Cell Biol. Int.* **34**, 645–653
  47. Blake, R. A., Broome, M. A., Liu, X., Wu, J., Gishizky, M., Sun, L., and Courtneidge, S. A. (2000) SU6656, a selective Src family kinase inhibitor, used to probe growth factor signaling. *Mol. Cell. Biol.* **20**, 9018–9027
  48. Toyoshima, F., and Nishida, E. (2007) Spindle orientation in animal cell mitosis: roles of integrin in the control of spindle axis. *J. Cell. Physiol.* **213**, 407–411
  49. Ditchfield, C., Johnson, V. L., Tighe, A., Ellston, R., Haworth, C., Johnson, T., Mortlock, A., Keen, N., and Taylor, S. S. (2003) Aurora B couples chromosome alignment with anaphase by targeting BubR1, Mad2, and Cenp-E to kinetochores. *J. Cell Biol.* **161**, 267–280

50. Liu, L., Tommasi, S., Lee, D. H., Dammann, R., and Pfeifer, G. P. (2003) Control of microtubule stability by the RASSF1A tumor suppressor. *Oncogene* **22**, 8125–8136
51. Wu, G., Lin, Y. T., Wei, R., Chen, Y., Shan, Z., and Lee, W. H. (2008) HICE1, a novel microtubule-associated protein required for maintenance of spindle integrity and chromosomal stability in human cells. *Mol. Cell Biol.* **28**, 3652–3662
52. Jackman, M., Lindon, C., Nigg, E. A., and Pines, J. (2003) Active cyclin B<sub>1</sub>-Cdk1 first appears on centrosomes in prophase. *Nat. Cell Biol.* **5**, 143–148
53. Buss, J. E., and Sefton, B. M. (1985) Myristic acid, a rare fatty acid, is the lipid attached to the transforming protein of Rous sarcoma virus and its cellular homolog. *J. Virol.* **53**, 7–12
54. Kaplan, J. M., Varmus, H. E., and Bishop, J. M. (1990) The Src protein contains multiple domains for specific attachment to membranes. *Mol. Cell Biol.* **10**, 1000–1009
55. Pérez, Y., Gairi, M., Pons, M., and Bernadó, P. (2009) Structural characterization of the natively unfolded N-terminal domain of human c-Src kinase: insights into the role of phosphorylation of the unique domain. *J. Mol. Biol.* **391**, 136–148
56. Pulvirenti, T., Giannotta, M., Capestrano, M., Capitani, M., Pisanu, A., Polishchuk, R. S., San Pietro, E., Beznoussenko, G. V., Mironov, A. A., Turacchio, G., Hsu, V. W., Sallese, M., and Luini, A. (2008) A traffic-activated Golgi-based signaling circuit coordinates the secretory pathway. *Nat. Cell Biol.* **10**, 912–922
57. Kinoshita, K., Noetzel, T. L., Pelletier, L., Mechtler, K., Drechsel, D. N., Schwager, A., Lee, M., Raff, J. W., and Hyman, A. A. (2005) Aurora A phosphorylation of TACC3/maskin is required for centrosome-dependent microtubule assembly in mitosis. *J. Cell Biol.* **170**, 1047–1055
58. Wang, L. H., Yan, M., Xu, D. Z., Cao, J. X., Zhu, X. F., Zeng, Y. X., and Liu, Q. (2008) Requirement of Aurora A kinase in astral microtubule polymerization and spindle microtubule flux. *Cell Cycle* **7**, 1104–1111
59. Borysova, M. K., Cui, Y., Snyder, M., and Guadagno, T. M. (2008) Knockdown of B-Raf impairs spindle formation and the mitotic checkpoint in human somatic cells. *Cell Cycle* **7**, 2894–2901
60. Tamemoto, H., Kadowaki, T., Tobe, K., Ueki, K., Izumi, T., Chatani, Y., Kohno, M., Kasuga, M., Yazaki, Y., and Akanuma, Y. (1992) Biphasic activation of two mitogen-activated protein kinases during the cell cycle in mammalian cells. *J. Biol. Chem.* **267**, 20293–20297
61. Heider, H., Hug, C., and Lucocq, J. M. (1994) A 40-kDa myelin basic protein kinase, distinct from Erk1 and Erk2, is activated in mitotic HeLa cells. *Eur. J. Biochem.* **219**, 513–520
62. Taylor, S. J., and Shalloway, D. (1996) Cell cycle-dependent activation of Ras. *Curr. Biol.* **6**, 1621–1627
63. Horne, M. M., and Guadagno, T. M. (2003) A requirement for MAP kinase in the assembly and maintenance of the mitotic spindle. *J. Cell Biol.* **161**, 1021–1028
64. O'Connell, C. B., and Wang, Y. L. (2000) Mammalian spindle orientation and position respond to changes in cell shape in a dynein-dependent fashion. *Mol. Biol. Cell* **11**, 1765–1774
65. Morin, X., and Bellaïche, Y. (2011) Mitotic spindle orientation in asymmetric and symmetric cell divisions during animal development. *Dev. Cell* **21**, 102–119